Yeast Nuclear Envelope Proteins Cross React with an Antibody against Mammalian Pore Complex Proteins

John P. Aris and Günter Blobel

Laboratory of Cell Biology, Howard Hughes Medical Institute, Rockefeller University, New York 10021

Abstract. We have used a monoclonal antibody raised against rat liver nuclear proteins to study two cross-reactive proteins in the yeast nucleus. In rat liver, this monoclonal antibody, mAb 414, binds to nuclear pore complex proteins, including one of molecular weight 62,000 (Davis, L. I., and G. Blobel. 1987. *Proc. Natl. Acad. Sci. USA.* 84:7552–7556). In yeast, mAb 414 cross reacts by immunoblotting with two proteins that have apparent molecular weights of 110,000 and 95,000, and are termed p110 and p95, respectively. Examination of subcellular fractions by immunoblotting shows that both p110 and p95 are located exclusively in the nuclear fraction. The mAb 414 immunoprecipitates several proteins from a crude yeast cell extract, including p110, p95, and a ~55-kD protein. Immunoprecipitation from subcellular fractions yields only p110 and p95 from purified nuclei, whereas the ~55-kD protein is immunoprecipitated from the soluble fraction. Digestion of purified nuclei with DNase to produce nuclear envelopes releases some of p110, but the majority of p110 is solubilized only after treatment of envelopes with 1 M NaCl. Immunofluorescence localization using yeast cells and isolated nuclei shows a punctate and patchy staining pattern of the nucleus. Confocal laser scanning immunofluorescence microscopy resolves the punctate and patchy staining pattern better and shows regions of fluorescence at the nuclear envelope. Postembedding immunogold electron microscopy using purified nuclei and mAb 414 shows colloidal gold decoration of the yeast nuclear envelope, but resolves pore complexes too poorly to achieve further ultrastructural localization. Immunogold labeling of nuclei followed by embedding suggests decoration of pore complexes. Thus, p110 and/or p95 are localized to the nuclear envelope in yeast, and may be components of the nuclear pore complex.

To a large extent, the nucleus is defined as an organelle by a boundary known as the nuclear envelope, which consists of an inner and outer membrane and pore complexes. The two membrane bilayers of the nuclear envelope unite at nuclear pores, yet each retains specific structural and functional specializations. The inner membrane is linked to the nuclear lamina (8, 12, 21, 29). The outer membrane is enriched in certain enzymes, such as HMG-CoA reductase, for example, in both higher and lower eucaryotes (24, 30). The nuclear pores contain large, protein-containing structures known as pore complexes (8). The pore complex is known to mediate and regulate the vectorial transport of protein and RNA molecules into and out of the nucleus (5, 6). In this way, the pore complex provides a channel for molecular communication between the nucleoplasm and cytoplasm. Many aspects of the biology of the nuclear envelope have been addressed (see reviews in references 5, 12, 15, 17, 20, 21).

The pore complex is a large supramolecular structure, having a diameter of ~70–100 nm, and its dimensions appear to be conserved across many phyla (17). One of the salient features of pore ultrastructure is its distinct eightfold symmetry when viewed *en face* (8, 26). Recently, the structure of the pore complex has been determined at a resolution of ~9 nm (26). The pore complex contains an aqueous channel, which has a functional diameter of ~11 nm, based on the measurement of diffusion of molecules through the pore (16). The transport of proteins >~40 kD across the pore is thought to involve a mechanism that recognizes nuclear targeting sequence information (5, 16). With an estimated mass of 25–50 × 10^6 D, the pore complex is thought to contain many protein, as well as RNA, components (12, 25).

A number of protein components of the pore complex have been identified in higher eucaryotes. A membrane glycoprotein, gp190, was identified in rat liver, and may serve to anchor the pore complex in the nuclear envelope (13). The primary structure of this glycoprotein has been determined recently (29a). A pore complex protein of 62,000 molecular weight, p62, has been identified using monoclonal antibodies (3, 4) and an assay for pore function (7). p62 is a member of a family of proteins that are posttranslationally modified with O-linked *N*-acetyl-glucosamine (3, 4, 7, 10, 11, 25). Certain monoclonal antibodies against pore complex proteins may recognize an epitope containing this sugar (3, 11, 23, 25). The inhibition of macromolecular transport across the pore with wheat germ agglutinin suggests a direct role

for p62 in pore function (7). The family of pore proteins that are characterized by this saccharide linkage includes proteins covering a broad range of relative molecular mass: 62–270 kD (3, 4); 45–210 kD (11, 25); or 35–110 kD (23).

Pore complexes in actively growing yeast cells appear to have a normal diameter (~100 nm), and are present at a frequency (~11 pores/μm^2) identical to that in many other cell types (14, 18). Interestingly, slow growth or growth arrest results in fewer pores per nucleus or an increase in pore diameter (14, 28). Pore synthesis during interphase of the yeast cell cycle may be comparable to that in higher eucaryotes (14, 19, 22). In addition, yeast provides an opportunity to study a nuclear envelope and pore complex that do not appear to disassemble during "closed" mitosis (2, 9). The identification of pore complex proteins in rat liver has provided us with an experimental approach to studying this structure in yeast (3, 4). We have used a monoclonal antibody that recognizes p62 to search for cross-reactive proteins in the yeast nucleus. As a result, we have identified two new proteins localized to the yeast nuclear envelope, and present evidence that these proteins may be further localized to nuclear pore complexes.

Materials and Methods

Yeast Strains, Reagents, and Materials

The protease-deficient haploid *Saccharomyces cerevisiae* strain BJ2168 (a, *prc1-407, prb1-1122, pep4-3, leu2, trp1, ura3-52*) was obtained from the Yeast Genetic Stock Center (Berkeley, CA). The standard Fleischmann's yeast strain was purchased at Sloan's Supermarket, New York. Lyticase, DNase I (type DN-EP), and 4',6-diamidino-2-phenylindole (DAPI)[1] were from Sigma Chemical Co. (St. Louis, MO). IgGsorb was from the Enzyme Center (Malden, MA). DL-dithiothreitol (DTT) and TX-100 were from Boehringer Mannheim Biochemicals (Indianapolis, IN). Affinity-purified goat anti-mouse 5- and 10-nm colloidal gold were obtained from Janseen Life Sciences Products (Piscataway, NJ). Fluorescein-conjugated goat anti-mouse antibody was from Organon Teknika-Cappel, (Malvern, PA). En^{3}Hance and ^{125}I-protein A (2–10 μCi/mg) were from Du Pont New England Nuclear Research Products (Wilmington, DE). Paraformaldehyde (EM grade), glutaraldehyde (EM grade), polylysine hydrobromide, and uranyl acetate were from Polysciences, Inc. (Warrington, PA). LR White (medium) embedding resin was from the London Resin Co., Ltd. (Surrey, England). Resin LX-112 was from Ladd Research Industries, Inc. (Burlington, VT). SDS was obtained from BDH Chemicals Ltd. (Poole, England). Ficoll 400 was from Pharmacia Fine Chemicals (Piscataway, NJ). All other chemicals, reagents, and media components were obtained from customary scientific vendors and were of high purity.

Purification of Nuclei

Nuclei were purified from the protease deficient strain BJ2168 as described (1), with the following modifications. Protease inhibitors were diluted from stock cocktails (1,000×) made in water (W) or DMSO (D) to final concentrations of: 1 mM ϵ-aminocaproic acid (W), 5 μg/ml aprotinin (W), 1 mM *p*-aminobenzamidine (W), 1 μg/ml chymostatin (D), 1 μg/ml leupeptin (W), 5 μg/ml pepstatin (D), 250 μM PMSF (D), and 50 μM *p*-chloromercuriphenyl sulfonic acid (D). The L, S, and H fractions harvested from the gradient used to purify nuclei were subjected to further purification than previously described (1). The L and H membrane fractions were diluted 1:10 with the 20% Ficoll buffer, homogenized, and centrifuged a second time for 1 h at 18,000 rpm in a rotor (model SW28; Beckman Instruments Inc., Palo Alto, CA) (1). The S fraction was centrifuged likewise without dilution. The L, H, and S fractions were harvested and stored at −80°C as described (1).

Digestion and Extraction of Nuclei

DNase I digestions and extractions were conducted as described (1), with modifications. Digestion with DNase was done in PMS buffer: 20 mM KP_i, pH 7.0, 0.1 mM $MgCl_2$, 250 mM sucrose. For extractions, nuclear envelopes were resuspended by homogenization in PES buffer: 20 mM KP_i, pH 7.0, 1 mM EDTA, 250 mM sucrose. Extraction with salt was done by adding an equal volume of PEN buffer: 20 mM KP_i, pH 7.0, 1 mM EDTA, 2 M NaCl. DTT (1 M) was freshly added to a final concentration of 1 mM in all buffers. Protease inhibitors were freshly added to the same final concentration used for the isolation of nuclei.

SDS-PAGE and Immunoblotting

SDS-PAGE was carried out with 8–14% gradient, or 10.5% polyacrylamide slab gels as described previously (1). For immunoblotting, proteins were electrophoretically transferred to nitrocellulose, and processing was done as previously described (1). The mAb 414 supernatant was diluted 1 in 20 with the standard immunoblotting buffer (1). Results were visualized by incubation with ^{125}I-protein A, followed by autoradiography.

Immunoprecipitation of ^{35}S-labeled Proteins from Yeast

For immunoprecipitations from lysates of whole yeast, strain BJ2168 was grown to an OD_{600} of 0.25 at 30°C in 20 ml of SD+ medium: 2% dextrose, 0.67% yeast nitrogen base without amino acids, plus 25 μg/ml of leucine, tryptophan, and uracil. The yeast were chilled on ice, washed twice, and resuspended in 4 ml of SD+ medium. Yeast were labeled for 90 min at 30°C after the addition of 0.4 mCi (0.36 nmol) of [^{35}S]methionine. Labeled yeast were chilled on ice and washed twice with cold IP buffer: 50 mM Tris, pH 7.5, 150 mM NaCl, 1 mM EDTA, 2 mM NaN_3. All buffers below contained protease inhibitors (see nuclei purification above). Yeast were resuspended in 0.2 ml of IP buffer plus 1% SDS, 1 mM DTT, and lysed by vortexing for 2 min in a 13 × 100-mm glass tube with 0.2 g of acid washed glass beads. The lysate was boiled 2 min, diluted with 0.8 ml of IP buffer plus 1% TX-100, 2 mM iodoacetamide, and placed on ice. The lysate was centrifuged at 500 *g* for 5 min, transferred to a microfuge tube and centrifuged at 12,000 *g* for 5 min at 4°C. The lysate was precleared in the cold for 1–2 h by transferring 1.0 ml to a microfuge tube containing 0.1 ml of washed and blocked IgGsorb. After a 10-min spin at 12,000 *g*, ~0.9 ml of supernatant was diluted 10-fold with IP buffer plus 1% TX-100, 0.2% SDS. Each immunoprecipitation was done with ~1 ml of the diluted lysate.

To purify ^{35}S-labeled nuclei, BJ2168 was grown in 100 ml of YPD at 30°C to an OD_{600} of 1.0. The yeast (~0.1 g) were washed twice with SP medium (without added amino acids; reference 1) and resuspended in 0.9 ml of SP medium containing 2 mM DTT, 0.4 mg Lyticase, and 2 mCi of [^{35}S]methionine. The yeast were labeled and digested for 60 min at 30°C. Nuclei were purified using a scaled down version of our previously described method (1). Instead of two spins in the rotor (model HB-4; Sorvall Instruments Div., Newton, CT), a single spin was done in a rotor (model TLS-55; Beckman Instruments Inc.) for 3 min at 12,000 rpm (12,300 g_{max}). A small aliquot of the supernatant was collected for the cleared lysate (CL) fraction. A 2.2-ml step gradient was centrifuged in the TLS-55 rotor for 15 min at 25,000 rpm (53,600 g_{max}). Purified nuclei and the soluble fraction were collected from the step gradient as usual. For immunoprecipitation, the crude lysate, soluble, or nuclear fractions (5 × 10^6 cpm each) were dissolved in a final volume of 0.2 ml of IP buffer plus 1% SDS, 2 mM DTT. Labeled nuclei were washed once in 20 mM KP_i, pH 6.5, 1 mM $MgCl_2$ before lysis. The samples were boiled 2 min and processed as described above. The precleared lysate was not diluted before use.

For each immunoprecipitation, 0.5 ml of the mAb 414 was preincubated with 15 μl of blocked protein G–Sepharose, and subsequently washed. The incubation with antibody was done overnight in the cold. The immunoprecipitate was washed sequentially at room temperature twice with: IP buffer plus 1% TX-100, 0.2% SDS; IP buffer plus 1% TX-100, 2 M urea: IP buffer alone. The samples were prepared for SDS-PAGE as usual after washing once with 10 vol of water. Gels were fluorographed with En^{3}Hance and placed against x-ray film.

Immunofluorescence Microscopy

A standard Fleischmann's yeast strain and strain BJ2168 were used according to methods previously described (1). Glutaraldehyde fixation was not done. The monoclonal supernatant was neutralized by adding 1 M Hepes acid to 25 mM. Fluorescein-conjugated goat anti-mouse antibody was preadsorbed with fixed, digested, permeabilized, and blocked yeast cells and applied at a final dilution of 1 in 200 (1). Specimens were observed with a Bio-Rad Lasersharp MRC-500 confocal laser scanning microscope, or a Zeiss Axiophot microscope using a 100× Plan-Neofluar objective, and images were recorded with Kodak Plus X or T-MAX film.

1. *Abbreviations used in this paper*: CLS, confocal laser scanning; DAPI, 4',6-diamidino-2-phenylindole.

Electron Microscopy

Nuclei were embedded in the hydrophilic resin LR White as previously described (1) after fixation with cold 3% *p*-formaldehyde and 0.2% glutaraldehyde in 50 mM KP_i, pH 6.5, 1 mM $MgCl_2$. Ultrathin sections on nickel grids were etched 15 min in fresh 10% $NaIO_4$. Incubations with antibody reagents and wash buffers were done as described (1) with the following modifications. All buffers contained TX-100 (0.01%). Before staining with uranyl acetate, the samples were cross-linked with 2% glutaraldehyde in PBS. Staining with Reynolds lead was omitted. For preembedding immunoelectron microscopy, purified nuclei suspended in Ficoll buffer (1) were fixed by diluting 10-fold with cold 20 mM KP_i, pH 6.5, 1 mM $MgCl_2$, 3% *p*-formaldehyde, 0.1% glutaraldehyde. Nuclei in fixative (1 ml/slide) were incubated in the cold overnight in multichambered slides (Titertek, Elfab Oy, Finland), previously coated with polylysine (1). The fixative solution was replaced by cold PBS, 1 mM $MgCl_2$, 3% *p*-formaldehyde, 0.1% glutaraldehyde, and fixation was continued 1 h. The slide was placed at room temperature for 1 h. The samples were washed three times with PBS with 1 mM $MgCl_2$, with 50 mM NH_4Cl in the second wash. Permeabilization with 0.1% TX-100 was done for 5 min at room temperature (1). Incubation with antibody reagents and washing buffers was done as described (1). Goat anti-mouse 5-nm colloidal gold was used at a 1:20 dilution. Conventional methods were used for fixation with glutaraldehyde, postfixation with osmium tetroxide, embedding in LX-112 resin, ultrathin sectioning, and staining (1). Specimens were visualized with a JEOL 100CX electron microscope at 60 kV, and photographs were recorded with Kodak electron microscope film.

Results

A Monoclonal Antibody against Rat Liver Pore Complex Proteins Recognizes Two Proteins in the Yeast Nucleus

The monoclonal antibody (mAb) 414 was previously shown to react with three proteins of M_r 62, 175, and 270 kD (3, 4). Results from immunofluorescence and immunoelectron microscopy demonstrated localization of the protein(s) to the pore complex in mammalian cells (3, 4). Our preliminary results suggested that at least one protein on immunoblots of yeast nuclear proteins cross-reacted with the 414 monoclonal antibody. Further analysis has shown that two proteins bind with high-affinity to mAb 414 on immunoblots of proteins from purified nuclei (Fig. 1 *A*). The apparent molecular masses on SDS gels of these two proteins are approximately 110,000 and 95,000 D. These two proteins are referred to as p110 and p95, respectively.

We examined the intracellular distribution of p110 and p95 by probing the cell fractions that result from the purification of yeast nuclei (1). These fractions are: purified nuclei (*N*); the low and high density membrane fractions (*L* and *H*); and the soluble fraction (*S*). The L, S, and H fractions are obtained from a yeast spheroplast lysate after Ficoll step gradient centrifugation (see Materials and Methods). Virtually all of the proteins of the yeast lysate are represented in the combination of these three fractions, with the exception of cell wall components. Immunoblotting shows that essentially all of p110 and p95 occur in the nuclear fraction (Fig. 1 *B*). The nonnuclear fractions L, S, and H do not contain detectable amounts of p110 or p95 (Fig. 1 *B*). Long exposures of the autoradiogram show that mAb 414 detects a protein of ~55 kD in the S fraction (not shown).

To extend the characterization of the cross-reactivity of mAb 414 in yeast, we did immunoprecipitation experiments. Using a crude lysate from [^{35}S]methionine-labeled yeast shows that mAb 414 immunoprecipitates a number of proteins, including bands of apparent mol wt 110,000 and 95,000 (Fig. 2, lane 2). A prominent protein band of ~55 kD was also immunoprecipitated (Fig. 2, lane 2). This band may include a group of proteins migrating close together in the SDS gel. To distinguish between nuclear and soluble proteins recognized by mAb 414, we did immunoprecipitations with subcellular fractions from labeled yeast. Nuclei were purified

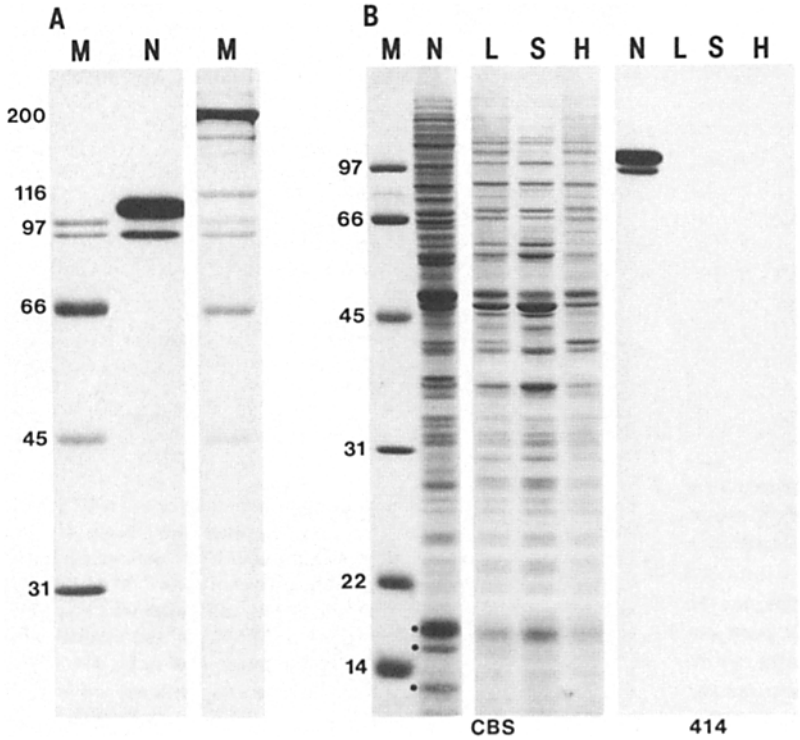

Figure 1. The monoclonal antibody 414 recognizes two proteins in the yeast nucleus. (*A*) Yeast nuclear proteins were separated by 8–14% gradient SDS-PAGE and probed by immunoblotting with mAb 414 (*N*). ^{14}C molecular mass standards ($M_r \times 10^{-3}$) were present on the immunoblot (*M*). (*B*) Yeast nuclear proteins (*N*, 100 μg), and the subcellular fractions L, S, H (33 μg) were separated by 10.5% SDS-PAGE and stained with Coomassie blue (*CBS*), or probed by immunoblotting as in *A* (*414*). The stained molecular mass standards are identical to those in *A* without the ^{14}C label. Histones are marked by dots.

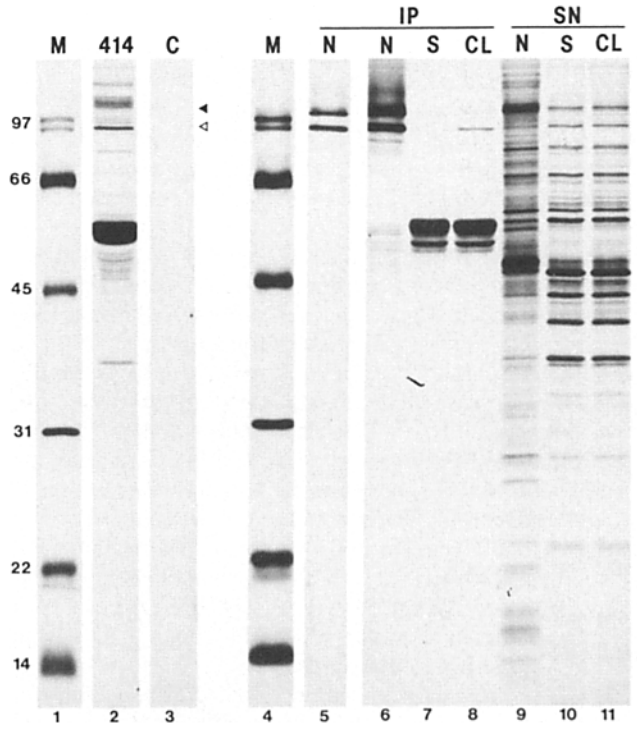

Figure 2. Immunoprecipitation of p110 and p95 with mAb 414. The immunoprecipitates obtained using mAb 414, or a control using no primary antibody (*C*), from an ^{35}S-labeled lysate of whole yeast are shown (lanes *2* and *3*). Immunoprecipitates from identical amounts (in cpm) of ^{35}S-labeled nuclei (*N*), soluble proteins (*S*), or a cleared lysate (*CL*), are shown (lanes *5–8*). Samples of the corresponding supernatants (*SN*) are equal to 1×10^{-3} of the original volume. Samples were electrophoresed on a 10.5% gel. Lanes *6–8* are from an overexposed fluorogram to show p110 and p95 in the *CL*, but not the *S*, fraction. Filled and open arrows point to p110 and p95. ^{14}C molecular mass standards are the same as in Fig. 1.

from [^{35}S]methionine-labeled yeast using a modified version of a previously described procedure (1). Immunoprecipitation was done using: purified nuclei (*N*); a soluble fraction (*S*); and a lysate cleared by a low speed centrifugation step (*CL*). The mAb 414 immunoprecipitates p110 and p95 from the nuclear fraction, but essentially none of the 55-kD protein(s), nor the minor band at 51 kD (Fig. 2, lanes *5–8*). The proteins between 50 and 55 kD are solely present in the immunoprecipitate from the soluble fraction, and none of p110 or p95 appear to coimmunoprecipitate with the 50–55-kD proteins.

Fractionation of Yeast Nuclei and the Disposition of p110

To investigate some of the intranuclear interactions involving p110 and p95, we fractionated nuclei using a method previously described (1). Digestion of nuclei with DNase in a buffer containing a low concentration of $MgCl_2$ is followed by centrifugation which separates nuclear envelopes into the pellet fraction. DNase digestion yields essentially pure nuclear envelopes, free of the majority of the chromatin, as indicated by the partitioning of ~90% of the histones into the supernatant fraction (Fig. 3). Approximately 70% of p110 is retained in the nuclear envelope fraction, with ~30% released by digestion with DNase (Fig. 3). The reduced detectability of p95 during fractionation of nuclei has been observed in more than one experiment, and the reason for this is not known. Envelopes washed with a high concentration of NaCl (1 M) are completely free of residual histones, and are substantially free of a number of other proteins, including the nucleolar protein p38 (1). The majority of p110 is found in the supernatant fraction after washing envelopes with a high salt buffer (Fig. 3). A small amount of p110 occurs in the salt-washed envelope fraction. Thus, the majority of p110 appears in the envelope and salt wash fractions, although the partitioning is not quantitative.

Immunofluorescence Localization in Yeast Cells and Purified Nuclei

With an interest in confirming the data from immunoblotting and immunoprecipitation, we did indirect immunofluorescence using the mAb 414. The immunofluorescence obtained with mAb 414 gives a distinctly nuclear pattern of staining in yeast cells (Fig. 4). Counter staining with DAPI clearly shows coincidence of the portion of the nucleus containing chromatin with the fluorescein signal. The area exhibiting

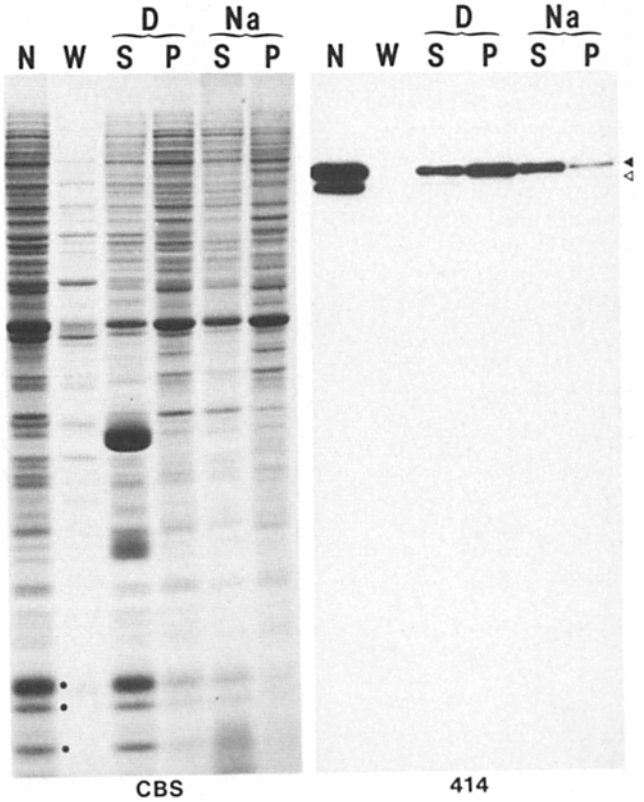

Figure 3. Subfractionation of purified nuclei. Nuclei (100 μg protein) were washed (*W*, wash fraction), digested with DNase (*D*), and centrifuged to generate a supernatant fraction (*S*) and nuclear envelopes (*P*). Nuclear envelopes were extracted with 1 M NaCl (*Na*) and centrifuged to give supernatant (*S*) and pellet (*P*) fractions. Samples were electrophoresed on a 10.5% gel and stained with Coomassie blue (*CBS*) or immunoblotted with mAb 414 (*414*). Filled and open arrows point to p110 and p95. Histones are marked by dots.

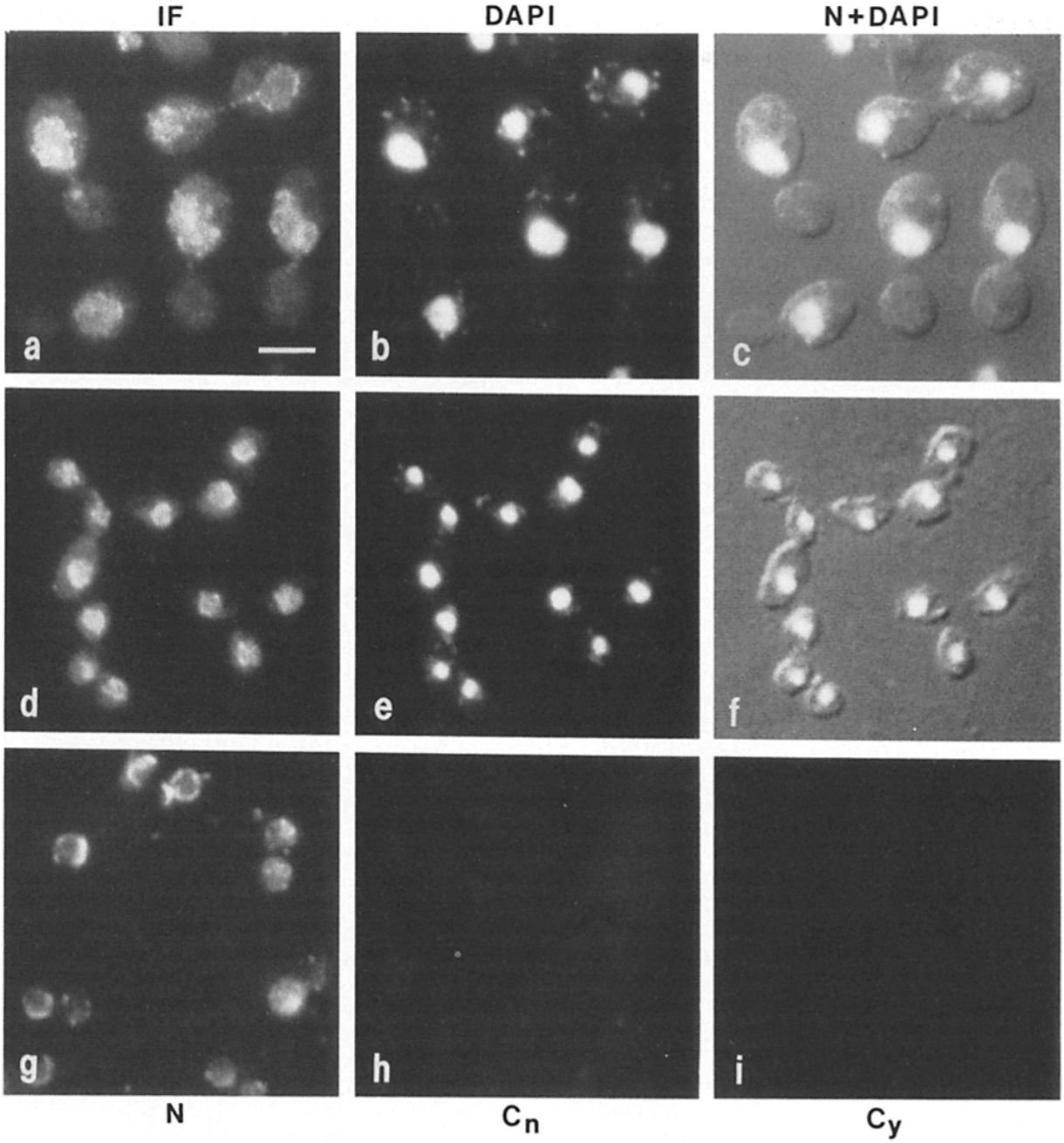

Figure 4. Immunofluorescence localization in yeast. Indirect immunofluorescence using mAb 414 and fluorescein-labeled secondary antibody was done using a standard method with Fleischmann's yeast (*a–c*, *i*), the haploid strain BJ2168 (*d–f*), or with isolated nuclei (*g* and *h*). The corresponding DAPI staining of chromatin (*b* and *e*) and the DAPI staining plus Nomarski optics image (*c* and *f*) are shown. Control panels of nuclei (C_n) or yeast cells (C_y) are from samples not treated with antibody (*h* and *i*). Bar, 4 μm.

immunofluorescence is greater than that seen with DAPI because a large portion of the nucleus is occupied by the nucleolus, which does not accumulate DAPI. In dividing pairs of yeast, the immunofluorescence extends through the bud neck between the chromatin masses (Fig. 4 *a*). The immunofluorescence localization with mAb 414 in the Fleischmann's yeast is identical to that seen in the haploid strain BJ2168 (Fig. 4, *d–f*). Strain BJ2168 has a smaller cell size, contains a small nucleus, and gives a correspondingly reduced distribution of immunofluorescence. Nuclei purified from BJ2168 show a fluorescence staining pattern comparable to that observed in the whole cells (Fig. 4, *g* and *h*). The fluorescence pattern is heterogeneous, with staining intensity at the nuclear envelope, as well as at the nuclear interior. In all nuclei many discrete points of fluorescence can be observed, in addition to larger patches of staining. A faint cytoplasmic staining is also visible in the yeast cells, and may correspond to the intracellular distribution of the soluble proteins recognized by mAb 414.

To visualize the immunofluorescence staining pattern in greater detail, a confocal laser scanning (CLS) microscope was used (Fig. 5). CLS microscopy offers improved resolu-

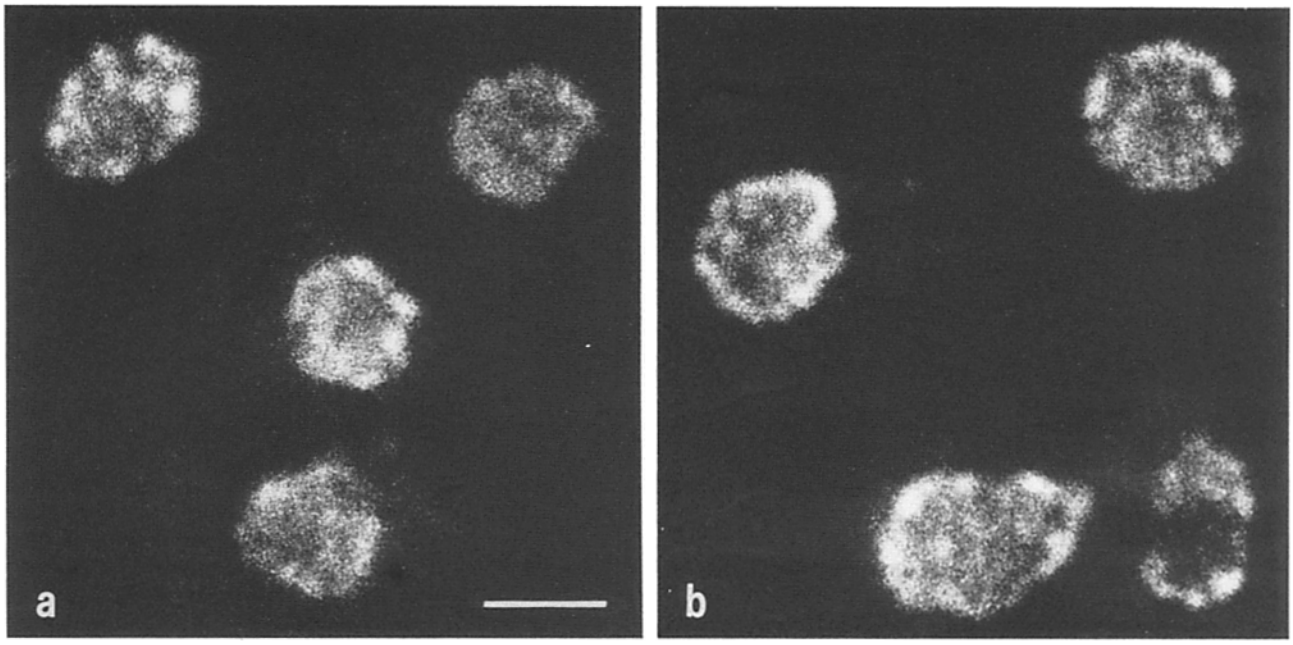

Figure 5. Confocal laser scanning immunofluorescence microscopy. Fleischmann's yeast were prepared as in Fig. 4. Two specimen fields at different focal planes are shown (*a* and *b*). The image was electronically magnified and enhanced. Bar, 4 μm.

tion of detail compared to standard microscopy because of the reduction of the out-of-focus epifluorescence above and below the focal plane (27). Examination of optical sections ~1.0 μm in thickness was coupled with limited electronic image enhancement to achieve optimal definition of staining features. This imaging system shows that the immunofluorescence is distributed in a fashion that appears both punctate and patchy, with notable fluorescence intensity located at the nuclear envelope (Fig. 5). We were unable to obtain images from optical sections <~1.0 μm in thickness because of the limited fluorescence intensity seen with the mAb 414. In addition, we found that the nucleus could be imaged with about two to three serial optical sections (not shown). This is probably due to flattening of the nucleus during preparation of yeast cells for microscopy.

These immunofluorescence findings are consistent with the immunoblotting and immunoprecipitation experiments. Moreover, yeast cells prepared for immunofluorescence experiments were harvested from a rapidly growing yeast culture. All stages of the cell cycle are present. Interestingly, different stages of the cell cycle show virtually identical staining patterns (Figs. 4 and 5). The punctate and patchy staining pattern was observed consistently in many fields of yeast cells examined (not shown). Hence, the distribution of the protein species that cross react with mAb 414 does not appear to undergo dramatic cell cycle specific changes.

Immunoelectron Microscopic Localization to the Nuclear Envelope

The fluorescence staining results suggested that mAb 414 reacted with the nuclear envelope, and that the discrete points of fluorescence may represent pore complex staining. To achieve ultrastructural localization, we embedded purified nuclei in the hydrophilic resin LR White and performed postembedding immunoelectron microscopy. Lowicryl was also used, but LR White gave the best preservation of the yeast epitope and was used routinely. Colloidal gold particles (10 nm) coated with a goat anti-mouse antibody serve as a marker for the distribution of mAb 414.

Postembedding immunoelectron microscopy with mAb 414 shows occurrence of gold particle label primarily over the nuclear envelope (Fig. 6, *a–e*). In typical control samples, where no mAb was used, no gold particles were observed over the nucleus (Fig. 6 *f*). Infrequently observed gold particles in control samples appeared to be distributed at random over the nucleus (not shown). The locations of gold particles in sections from 50 nuclei were surveyed, and the data collated. This analysis shows that the abundance of gold labeling occurs at the nuclear envelope (Fig. 7). The nuclei had an average diameter of ~1.6 μm. The average number of gold particles per nucleus was 4.42, with a range of 2–12.

In the postembedding experiment, a small number of gold particles were not positioned directly over the envelope, but were located within 60 nm distance of either side of the nuclear envelope (Fig. 7). We have observed that the envelope is not always preserved intact in nuclei prepared for electron microscopy. Nuclei may have portions of the envelope separated from underlying chromatin or nucleolus (not shown). In addition, pore complexes are not readily visualized. In general, this may be due to the fact that the nuclear envelope and pore complexes in yeast are relatively fragile and/or poorly preserved.

To supplement the postembedding approach using LR White, we labeled nuclei before embedding and processed samples using standard methods. Pore complexes may be seen after nuclei are processed using standard methods for glutaraldehyde fixation, postfixation with osmium, and embedding in a hydrophobic resin (1). However, the preservation of pore complex morphology in yeast is not as good

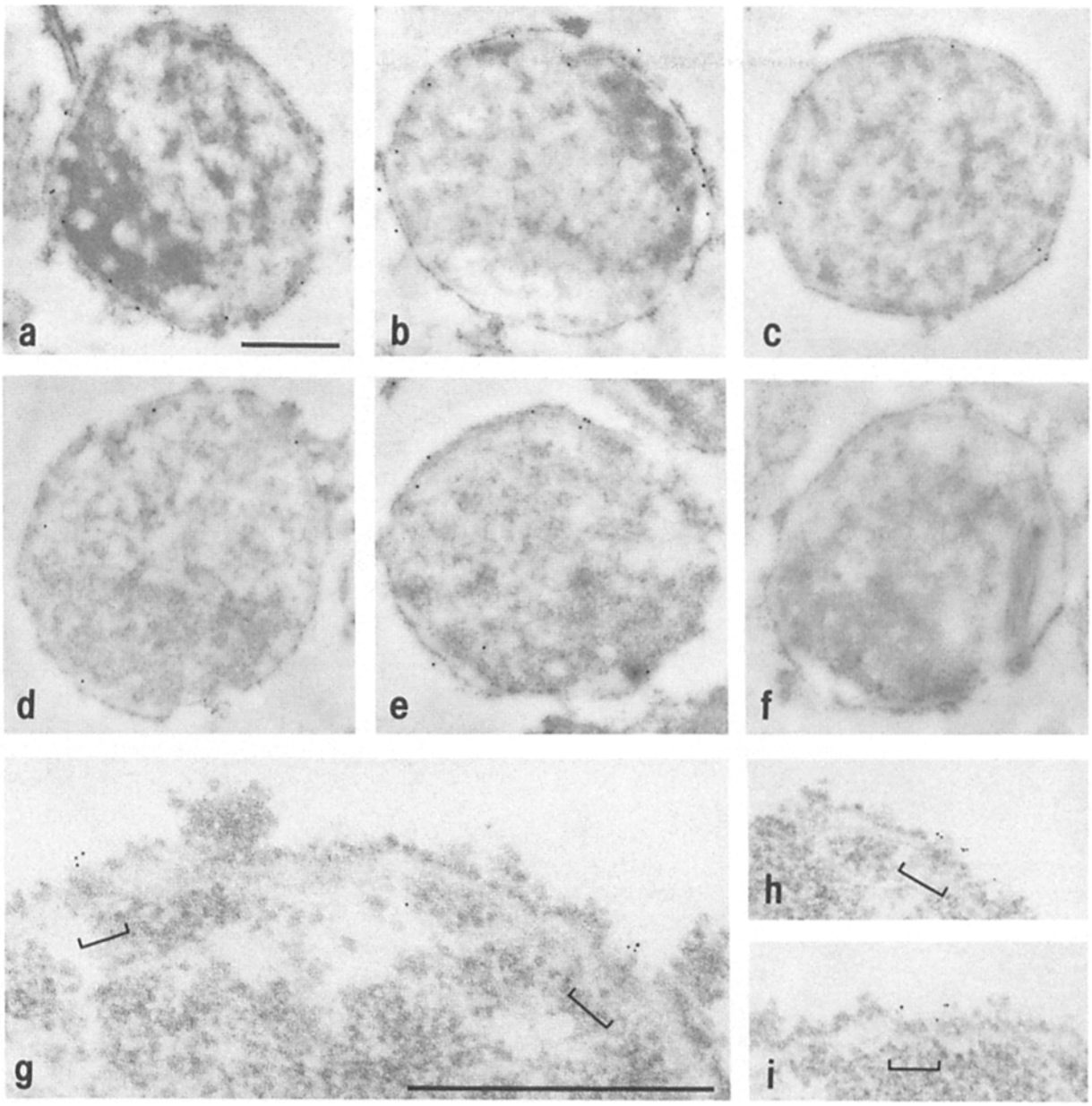

Figure 6. Immunolocalization electron microscopy. Postembedding immunogold labeling of nuclei embedded in LR White resin using mAb 414 and secondary antibody adsorbed to 10-nm colloidal gold particles shows decoration of the nuclear periphery (*a–e*). A control minus mAb 414 shows no decoration (*f*). Immunogold labeling of nuclei using 5-nm colloidal gold particles followed by standard processing and embedding shows decoration of pore complexes (*g–i*). Pore complexes are designated by brackets. Bars, 0.5 μm.

as that observed in higher eucaryotic cells. Nuclei were fixed, attached to dishes, permeabilized with TX-100, probed with antibody, and prepared for EM (Fig. 6, *g–i*). Treatment with TX-100 solubilizes the membranes of the nuclear envelope. The position of the outer membrane is marked by a row of ribosomes that remain. Pore complexes may be identified by virtue of their position in the envelope, dense staining property, and apparent diameter (~100 nm). Colloidal gold (5 nm) secondary antibody appears to decorate pore complexes and to localize the mAb 414 to these structures (Fig. 6, *g–i*). We note that although the majority of the pore complexes were decorated with colloidal gold, not every pore complex was labeled, and some of the colloidal gold particles appeared juxtaposed to the nuclear envelope.

Discussion

In this report, we have identified two proteins in the yeast nucleus, which cross-react with a monoclonal antibody that recognizes mammalian pore complex proteins. In rat liver nuclei, this monoclonal recognizes proteins of M_r 62, 175, and 270 kD and decorates pore complexes by immunoelectron microscopy (3, 4). We find that the two proteins of 110 and 95 kD, termed p110 and p95, are components of the yeast nucleus by immunoblotting and subcellular fractionation. These two polypeptides are not detectable by immunoblotting nonnuclear fractions including a cytosolic fraction, or fractions containing a mixture of membranes from the vacuole, plasma membrane, and endoplasmic reticulum. Immu-

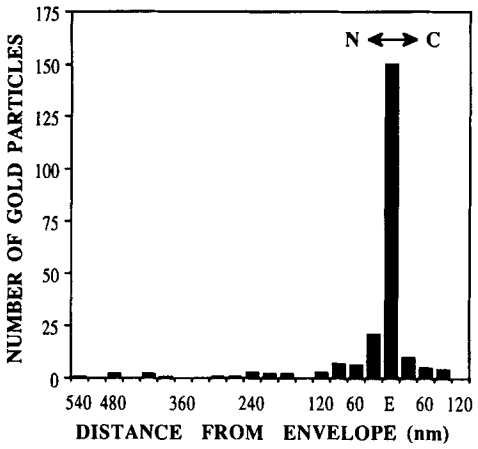

Figure 7. Distribution of immunogold label on yeast nuclei. The locations of colloidal gold particles were determined for sections of 50 nuclei subjected to postembedding immunogold labeling as in Fig. 6. The nuclear envelope (*E*) marks the zero distance point on the abscissa. The nuclear (*N*) and cytoplasmic (*C*) faces of the envelope are designated.

noprecipitation with mAb 414 from a crude radiolabeled yeast lysate shows that a number of proteins bind to mAb 414. The major proteins in the mAb 414 immunoprecipitate are p110, p95, and a ~55-kD protein or group of proteins. Immunoprecipitations from radiolabeled yeast cell subfractions show that p110 and p95 are exclusively localized in the nucleus, but that the ~55-kD protein(s) appear(s) in the cytosolic compartment.

Fractionation of nuclei demonstrates that the majority of p110 cosediments with the nuclear envelope fraction after DNase digestion, which releases the majority of the histones into the soluble fraction. p110 is released from nuclear envelopes by exposure to a high (1 M) salt concentration. Thus, p110 does not fractionate like an integral membrane protein. For unknown reasons, the detectability of p95 by immunoblotting was reduced during nuclear fractionation, and the fractionation behavior of this protein was not followed. The fractionation behavior of p110 does not exclude the possibility that p110 participates in interactions with other intranuclear proteins or structures. For example, the nucleolar protein p38 exhibits fractionation behavior similar to p110 (1). However, p110 shows fractionation properties similar to the rat liver pore complex protein p62, which is solubilized from nuclear envelopes with 0.5 M NaCl (3). The disposition of p110 in nuclear fractionation experiments is consistent with association of p110 with the yeast nuclear envelope.

Immunofluorescence microscopy with mAb 414 shows staining of the nucleus in yeast and a faint staining dispersed throughout the cytosol. The faint cytosolic staining probably corresponds to the intracellular distribution of the ~55-kD protein(s) recognized by mAb 414. The nuclear staining pattern most likely represents the intracellular location of p110 and/or p95. Identical results are obtained in polyploid and haploid yeast strains, and in isolated nuclei. The staining pattern appears qualitatively the same in cells in different stages of the cell cycle. The maintenance of a continuous nuclear envelope during closed mitosis in yeast argues that pore complex structure is maintained intact throughout mitosis as well (2, 9). The nuclear staining pattern obtained with mAb 414 is different from the crescent staining pattern diagnostic of components of the yeast nucleolus, such as p38 (1).

The small size of the yeast nucleus makes it difficult to resolve this fluorescence staining pattern. We used the CLS microscopic technique with mAb 414 to distinguish the punctate staining more clearly, and demonstrate preferential localization of fluorescence to regions of the nuclear envelope. CLS microscopy has been shown to produce high resolution immunofluorescence images (27). The punctate and patchy, partially rim staining pattern in yeast is similar to the punctate rim staining pattern observed in higher eucaryotic cells (3, 23, 25). This punctate rim staining in higher cells has been used as one criterion for the identification of pore complex proteins (3). The more discretely punctate immunofluorescence seen in animal cells in tissue culture is discerned at lower magnification. The poorer resolution of this punctate rim staining pattern in yeast is probably due to the fact that the yeast nucleus (2–6 μm in diameter) is much smaller than that in animal cells, and is partially flattened during specimen preparation for microscopy. By comparison, an image from a focal plane through the middle of an animal cell nucleus (20–50 μm in diameter) is more readily obtained.

Immunoelectron microscopy shows that mAb 414 recognizes proteins that are localized to the nuclear envelope in yeast. Considering the biochemical immunoreactivity of mAb 414, the most likely interpretation of the labeling of the nuclear envelope is that this is the location of p110 and/or p95 in the yeast nucleus. Moreover, labeling of structures resembling pore complexes suggests that p110 and/or p95 are components of the yeast pore complex. The immunogold labeling of pores may correspond to the punctate immunofluorescence observed. Localization of p110 and/or p95 to pores, a group of pores, or to the envelope may correspond to the punctate and patchy pattern of immunofluorescence.

Despite the examination of several variables in the preparation of nuclei for electron microscopy, pore complex morphology in isolated yeast nuclei is preserved relatively poorly compared to that obtained in higher eucaryotic cells, as judged by the two methods for immunoelectron microscopy that we have used. This may reflect suboptimal conditions for pore complex preservation during the isolation of nuclei or preparation for EM, or may suggest that the pore complex in yeast is relatively fragile. Perhaps, pore complexes in yeast are more "plastic" than their counterparts in higher cells due to, for example, the requirements of closed mitosis.

Proteins similar in mass to p110 and p95 have been reported in rat liver and Chinese hamster ovary (CHO) cells (23, 25). Snow et al. (25) have generated three monoclonal antibodies that react with a 100-kD protein, which is modified by O-linked *N*-acetyl-glucosamine, among others in rat liver nuclei. A monoclonal isolated by Park et al. (23) recognizes a 110-kD protein. However, considering that in a number of cases a single monoclonal recognizes a number of pore proteins spanning a broad range of molecular weights, it is improbable that homologies between yeast and mammalian pore complex proteins can be assigned on the basis of molecular weight alone. The pore complex proteins identified in mammalian cells appear to have in common the possession of one or more O-linked *N*-acetyl-glucosamine

residues (11). The sugar moiety contributes to the epitopes recognized by certain monoclonals, but is not the sole epitope (11). This raises the possibility that p110 and p95 in yeast are glycosylated in an analogous fashion. Preliminary results indicate that wheat germ agglutinin–Sepharose precipitates from radiolabeled yeast nuclei two proteins, among others, that comigrate on SDS gels with p110 and p95 (Aris and Blobel, unpublished results).

Further characterization of p110 and p95 will better define additional similarities, if any, between the yeast and mammalian proteins recognized by mAb 414. The production of antibody reagents specific for p110 and p95 will probably allow more definitive ultrastructural localization of these two polypeptides, as well as enabling us to distinguish between the individual properties of each protein. The identification of p110 and p95 suggests that certain domains of nuclear envelope proteins, and more specifically pore complex proteins, are identical in yeast and mammalian cells. Monoclonal antibodies directed against other mammalian pore proteins may cross-react with pore complex proteins from yeast, and provide insight into pore structure and function in both systems.

We are grateful to Dr. Laura Davis for providing the mAb 414 supernatant. We thank Mr. Raj Mundhe and Mr. Lloyd London at Bio-Rad Microscience Division for the use of the Bio-Rad Lasersharp MRC-500 confocal fluorescence imaging system. Ms. Eleana Sphicas provided expert assistance in sample preparation for electron microscopy.

J. P. Aris was supported by National Institutes of Health grant GM10506, and by the Howard Hughes Medical Institute.

Received for publication 20 December 1988 and in revised form 13 February 1989.

References

1. Aris, J. P., and G. Blobel. 1988. Identification and characterization of a yeast nucleolar protein that is similar to a rat liver nucleolar protein. *J. Cell Biol.* 107:17–31.
2. Byers, B. 1981. Cytology of the yeast life cycle. *In* The Molecular Biology of the Yeast *Saccharomyces*: Life Cycle and Inheritance. J. N. Strathern, E. W. Jones, and J. R. Broach, editors. Cold Spring Harbor Laboratory, Cold Spring Harbor, NY. 59–96.
3. Davis, L. I., and G. Blobel. 1986. Identification and characterization of a nuclear pore complex protein. *Cell.* 45:699–709.
4. Davis, L. I., and G. Blobel. 1987. Nuclear pore complex contains a family of glycoproteins that includes p62: glycosylation through a previously unidentified cellular pathway. *Proc. Natl. Acad. Sci. USA.* 84:7552–6.
5. Dingwall, C., and R. A. Laskey. 1986. Protein import into the cell nucleus. *Annu. Rev. Cell Biol.* 2:367–90.
6. Dworetzky, S. I., and C. M. Feldherr. 1988. Translocation of RNA-coated gold particles through the nuclear pores of oocytes. *J. Cell Biol.* 106:575–84.
7. Finlay, D. R., D. D. Newmeyer, T. M. Price, and D. J. Forbes. 1987. Inhibition of in vitro nuclear transport by a lectin that binds to nuclear pores. *J. Cell Biol.* 104:189–200.
8. Franke, W. W. 1974. Structure, biochemistry, and functions of the nuclear envelope. *Int. Rev. Cytol.* 4(suppl.):72–236.
9. Heath, I. B. 1980. Variant mitoses in lower eukaryotes: indicators of the evolution of mitosis? *Int. Rev. Cytol.* 64:1–80.
10. Holt, G. D., and G. W. Hart. 1986. The subcellular distribution of terminal *N*-acetylglucosamine moieties. *J. Biol. Chem.* 261:8049–57.
11. Holt, G. D., C. M. Snow, A. Senior, R. S. Haltiwanger, L. Gerace, and G. W. Hart. 1987. Nuclear pore complex glycoproteins contain cytoplasmically disposed O-linked *N*-acetylglucosamine. *J. Cell Biol.* 104: 1157–64.
12. Gerace, L., and B. Burke. 1988. Functional organization of the nuclear envelope. *Annu. Rev. Cell Biol.* 4:335–74.
13. Gerace, L., Y. Ottaviano, and C. Kondor-Koch. 1982. Identification of a major polypeptide of the nuclear pore complex. *J. Cell Biol.* 95:826–837.
14. Jordan, E. G., N. J. Severs, and D. H. Williamson. 1977. Nuclear pore formation and the cell cycle in *Saccharomyces cerevisiae*. *Exp. Cell Res.* 104:446–9.
15. Kessel, R. G. 1988. The contribution of the nuclear envelope to eukaryotic cell complexity: architecture and functional roles. *CRC Crit. Rev. Anat. Cell Biol.* 1:327–423.
16. Lang, I., M. Scholz, and R. Peters. 1986. Molecular mobility and nucleocytoplasmic flux in hepatoma cells. *J. Cell Biol.* 102:1183–90.
17. Maul, G. G. 1977. The nuclear and cytoplasmic pore complex: structure, dynamics, distribution, and evolution. *Int. Rev. Cytol.* 6(suppl.):75–186.
18. Maul, G. G., and L. Deaven. 1977. Quantitative determination of nuclear pore complexes in cycling cells with differing DNA content. *J. Cell Biol.* 73:748–60.
19. Maul, G. G., H. M. Maul, J. E. Scogna, M. W. Lieberman, G. S. Stein, B. Y.-L. Hsu, and T. W. Borun. 1972. Time sequence of nuclear pore formation in phytohemagglutinin-stimulated lymphocytes and in HeLa cells during the cell cycle. *J. Cell Biol.* 55:433–47.
20. Newport, J. W., and D. J. Forbes. 1987. The nucleus: structure, function, and dynamics. *Annu. Rev. Biochem.* 56:535–65.
21. Nigg, E. A. 1988. Nuclear function and organization: the potential of immunochemical approaches. *Int. Rev. Cytol.* 110:27–92.
22. Ottaviano, Y., and L. Gerace. 1985. Phosphorylation of the nuclear lamins during interphase and mitosis. *J. Biol. Chem.* 260:624–632.
23. Park, M. K., M. D'Onofrio, M. C. Willingham, and J. A. Hanover. 1987. A monoclonal antibody against a family of nuclear pore proteins (nucleoporins): O-linked *N*-acetylglucosamine is part of the immunodeterminant. *Proc. Natl. Acad. Sci. USA.* 84:6462–6.
24. Pathak, R. K., K. L. Luskey, and R. G. W. Anderson. 1986. Biogenesis of the crystalloid endoplasmic reticulum in UT-1 cells: evidence that newly formed endoplasmic reticulum emerges from the nuclear envelope. *J. Cell Biol.* 102:2158–68.
25. Snow, C. M., A. Senior, and L. Gerace. 1987. Monoclonal antibodies identify a group of nuclear pore complex glycoproteins. *J. Cell Biol.* 104:1143–56.
26. Unwin, P. N. T., and R. A. Milligan. 1982. A large particle associated with the perimeter of the nuclear pore complex. *J. Cell Biol.* 93:63–75.
27. White, J. G., W. B. Amos, and M. Fordham. 1987. An evaluation of confocal versus conventional imaging of biological structures by fluorescence light microscopy. *J. Cell Biol.* 105:41–8.
28. Willison, J. H. M., and G. C. Johnston. 1978. Altered nuclear pore diameters in G1-arrested cells of the yeast *Saccharomyces cerevisiae*. *J. Bacteriol.* 136:318–23.
29. Worman, H. J., J. Yuan, G. Blobel, and S. D. Georgatos. 1988. A lamin B receptor in the nuclear envelope. *Proc. Natl. Acad. Sci. USA.* 85:8531–34.
29a. Wozniak, R. W., E. Bartnik, and G. Blobel. 1989. Primary structure analysis of an integral membrane glycoprotein of the nuclear pore. *J. Cell Biol.* 108:2083–2092.
30. Wright, R., M. Basson, L. D'Ari, and J. Rine. 1988. Increased amounts of HMG-CoA reductase induce "karmellae": a proliferation of stacked membrane pairs surrounding the yeast nucleus. *J. Cell Biol.* 107:101–14.